Nanotechnology **18** (2007) 215602 (5pp) doi:10.1088/0957-4484/18/21/215602

Growth of self-assembled ZnO nanoleaf from aqueous solution by pulsed laser ablation

Li Yang[1,4], Paul W May[1], Lei Yin[2] and Tom B Scott[3]

[1] School of Chemistry, University of Bristol, Cantock's Close, Bristol BS8 1TS, UK
[2] Department of Aerospace Engineering, University of Bristol, Queen's Building, University Walk, Bristol BS8 1TR, UK
[3] Interface Analysis Centre, University of Bristol, Oldbury House, 121 St Michael's Hill, Bristol BS2 8BS, UK

E-mail: li.yang@bristol.ac.uk

Received 19 February 2007, in final form 23 March 2007
Published 27 April 2007
Online at stacks.iop.org/Nano/18/215602

Abstract
Zinc oxide 'nanoleaf' structures have been synthesized at room temperature and pressure using the novel technique of pulsed laser ablation (Nd:YAG 532 nm) of a zinc target in an aqueous solution of sodium dodecyl sulfate (SDS). Transmission electron microscopy (TEM), selected area electron diffraction (SAED), high-resolution transmission electron microscopy (HRTEM), photoluminescence spectroscopy and UV–visible spectroscopy were used to study the morphology, nanostructure and optical properties of these ZnO nanostructures. The growth mechanism appears to involve an increase of the structural complexity from zero-dimensional nanoparticles to one-dimensional nanorods, and then broadening of these into two-dimensional 'nanoleaf' structures. Variations are discussed in terms of differences in the concentration of SDS and the laser ablation time.

(Some figures in this article are in colour only in the electronic version)

1. Introduction

Over the past decade, pulsed laser ablation at the solid–liquid interface has aroused intense interest [1, 2]. This novel technique is known as liquid phase pulsed laser ablation (LP-PLA), and it involves the firing of laser pulses through liquids transparent to that wavelength onto a target substrate. The ablation plume interacts with the surrounding liquid particles creating cavitation bubbles, which upon their collapse, give rise to extremely high pressures and temperatures. These conditions are, however, very localized and exist across the nanometre scale. Indeed, LP-PLA has proven to be an effective method for preparation of many nanostructured materials, including nanocrystalline diamond [3], cubic boron nitride [4], and nanometre-sized particles of Ti [5], Ag [6], Au [7] and TiC [8].

Recently, the LP-PLA technique has been applied to zinc oxide by using a Zn target and an aqueous solution containing different surfactants. These surfactants stick to the charged particle surfaces, preventing further growth, and thereby aid the production of small particle sizes. For instance, Usui and co-workers [9] used the surfactant cetyltrimethylammonium bromide (CTAB), lauryl dimethylaminoacetic (LDA) and octaethylene glycol monododecyl (OGM) to help form ZnO nanoparticles (NPs) with an average size of 12 nm. Also, Zeng and co-workers [10] used a solution of sodium dodecyl sulfate (SDS) to produce ∼20 nm Zn/ZnO core–shell structure particles. These reports show that ZnO mainly forms zero-dimensional (0D) NPs by LP-PLA, although various approaches, including chemical vapour deposition, thermal evaporation, template-involved processes and solution-phase synthesis, have been employed successfully for preparing more complex two-dimensional (2D) and three-dimensional (3D) superstructures of ZnO [11, 12]. However, to the best of our knowledge, use of the LP-PLA technique has not yet been reported for the self-assembly of such complex ZnO structures.

[4] Author to whom any correspondence should be addressed.

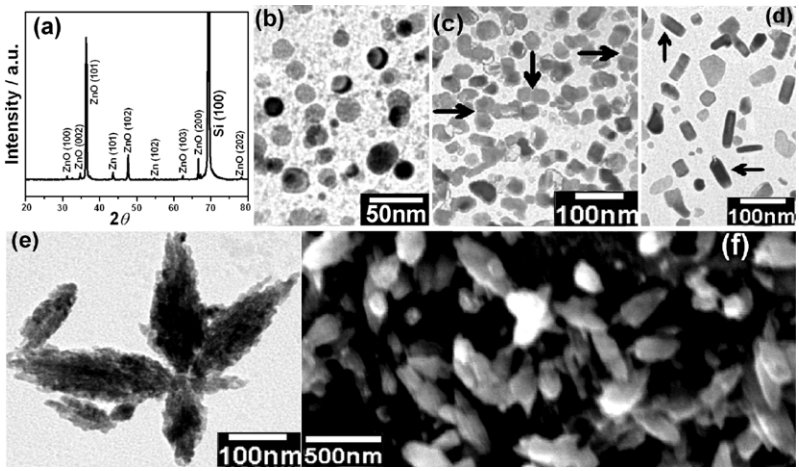

Figure 1. (a) Representative XRD pattern for the LP-PLA product (0.01 M SDS, $t = 2$ h). TEM images of the samples ablated with 0.01 M SDS for different ablation times (b) 0.5 h, (c) 2 h, (d) 2.5 h and (e) 5 h. (b) Spherical nanoparticles with a particle size of ∼5–25 nm. (c) Adjacent particles that are aligned with one another are highlighted by arrows. (d) Nanorods (highlighted by arrows) which might be formed by NP 1D growth. (e) Well-developed 'leaf-like' structures with rough and dense surfaces. (f) SEM image of ZnO nanoleaf structures prepared by 0.01 M SDS and 5 h ablation times.

Our recent findings [13–16] indicated that the instantaneous high temperature, high pressure and high density conditions that arise during LP-PLA can promote growth of crystalline carbon nitride nanomaterials. We demonstrated that the nanocrystals self-assemble into complex 2D and 3D architectures. In this paper, a similar synthesis for new, complex 2D nanostructures of zinc oxide is reported, using an aqueous solution of SDS. This surfactant was chosen because it has been widely used in other systems, and it is known to affect the initial self-assembly process and also modify the resulting particle morphology [17].

2. Experimental details

99.99% Zn powder was compressed under (∼10 kg cm^{-2}) pressure to form a solid target for ablation. Different ZnO nanostructures were prepared by LP-PLA in an aqueous solution with anionic surfactant SDS in a volume of 5 ml, using apparatus and methods that have been described in detail elsewhere [13]. Briefly, the laser beam was a Nd:YAG (532 nm, pulse duration 15 ns, frequency 10 Hz) with the power kept constant at 100 mJ per pulse, and focused through ∼5 mm of the liquid onto a 0.5 mm diameter spot on the ZnO target surface. All the laser ablation experiments were performed at room temperature and 1 atmosphere pressure. Different SDS concentrations (0.05–0.001 M) and ablation times, t, (0.5–5 h) were investigated. After ablation, the product was visible as a suspension of grey nanoparticles in the liquid. In order to remove traces of SDS, the grey precipitates were washed several times with deionized water and ethanol, and then separated by centrifugation. The solid precipitate samples were characterized and analysed by scanning electron microscopy (SEM, JEOL 6300LV), transmission electron microscopy (TEM, JEOL 1200EX) and high-resolution (HR) TEM (JEOL 2010). Powder x-ray diffraction (XRD, Bruker-AXS D8 Powder Diffractometer) and selected area electron diffraction (SAED) were used to identify the zinc oxide phases. Wavelength-dispersed photoluminescence (PL) spectra were measured at room temperature following excitation with a cw He–Cd laser ($\lambda = 325$ nm, power ∼3 mW). An ultraviolet–visible (UV–vis) spectrophotometer (Perkin-Elmer Lamda 11) was used to monitor the changes in absorbance of the ablated solution.

3. Results and discussion

As laser irradiation progressed, the liquid changed from colourless to a grey coloured suspension, indicating an increase in solid product and/or a change in composition of the solid due to interaction with the laser. A typical XRD study in figure 1(a) shows that the prepared samples were consistent with the ZnO wurtzite phase ($P6_3mc$(186), JCPDS card no. 36-1451) with lattice constants $a_0 = 3.2498$ Å and $c_0 = 5.2066$ Å [18]. One-dimensional spherical particles (figure 1(b)) of size ∼5–25 nm appeared after only 30 min ablation in 0.01 M SDS. When increasing the laser ablation time to 2 h, the crystallites had elongated into rod-like structures, as shown in figure 1(c). The elongation mechanism is still unclear, but figure 1(c) shows some adjacent particles (highlighted by arrows) may be lining up. This suggests that the nanorods (NRs) may be the result of individual pre-formed NPs adding preferentially to the ends of a line of NPs (figure 1(d)). Alternatively, NRs may form by 1D growth of a single NP, but we have not yet found any evidence for this. Whichever mechanism is correct, it is clear that NR formation, growth and aggregation all occur after only a short ablation time. This is consistent with the findings of Zeng *et al* [19], who observed NPs of ZnO after short-duration LP-PLA.

For longer ablation times, new 'leaf-like' shapes were observed (width: 230 ± 30 nm, length: 770 ± 90 nm), as shown in figure 1(e). This image provides evidence of oriented attachment growth, and that the ZnO leaf matrix is composed of many NPs attached side-by-side. A similar phenomenon was also observed by other workers in undoped ZnO NRs, hollow microhemispheres [20] and co-doped ZnO nanosheet-based structures [21]. Noticeably, the individual leaf-like structures within a local region seem to be randomly

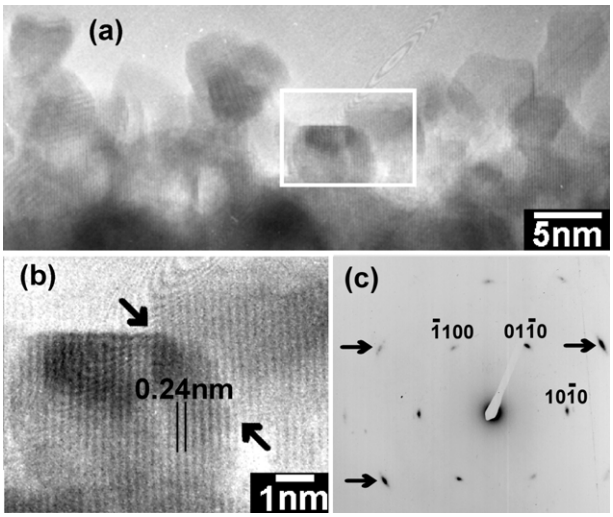

Figure 2. (a) HRTEM image of a series of aggregated ZnO NPs, (b) adjacent particles from the framed area in (a) showing aligned orientations and lattice fringes. The arrows point to the boundaries between the crystallites. (c) SAED pattern taken from the framed area in (a) observed along the [0001] zone axis, which is consistent with hexagonal symmetry. The arrows point to the curvature of the diffraction spots.

oriented, while the NPs are aligned preferentially parallel to the *c* axis along the leaf. Again, it was found that these leaf-like nanostructures are mostly made up of component NPs or NRs, as shown in the SEM image (figure 1(f)).

The HRTEM image in figure 2(a) shows that the individual NPs contain very few defects and are primarily faceted with $\{10\bar{1}1\}$ crystal planes (see the enlarged image of the framed area in figure 2(a)), as anticipated from the XRD pattern. The clear lattice fringes ($d_{10\bar{1}1} = 0.24$ nm) obtained from all crystallites are in good agreement with the values for hexagonal ZnO [18]. The ZnO crystalline NPs that build the leaf-like structures are consistent with an 'oriented attachment' mechanism [22], whereby the adjacent ZnO building units are perfectly aligned with each other in a close orientation relationship, with no mismatch (as shown in figure 2(b), highlighted by arrows between the boundaries). This explains the reason for the slight curvature of the diffraction spots observed in the SAED pattern (figure 2(c), taken from the framed area in (a)).

In our experiments, the formation of the distinct leaf-like morphology is very sensitive to the reaction conditions. Concentrations of SDS near the critical micelle concentration (cmc = 0.008 M) and longer ablation times, both favour formation of the leaf-like structures. For lower SDS concentrations (0.001 M) and shorter ablation times (2 h), instead of rod-like particles (as in figure 1(c)), the zinc oxide formed 0D spheres or aligned spheres (figures 3(a), (b)). For higher SDS concentrations (0.05 M > cmc) and the same ablation time, the product contained a mixed collection of NPs and NRs (figure 3(c)). Many 0D nanocrystallites have coalesced into straight rod-like structures (shown by the arrows), as further evidence for the proposed growth mechanism. However, on increasing the ablation time to 5 h, the NRs aggregated into leaf-like particles (figure 3(d)). The resulting nanoleaf (width: 200±40 nm, length: 500±80 nm) is smaller than the ones produced in 0.01 M SDS. This shows that the morphology of the nanostructures is dependent upon the SDS concentration. It is known [23] from studies of $Zn(OH)_2$ NPs that SDS molecules can form a layer directly on a particle surface, which helps to limit the particle size to the nanometre range. The negative sulfate groups attach to the positive NP surface, leaving the hydrocarbon tails unbound in the liquid. Close to and above the cmc, it becomes energetically favourable for the tails from different NPs to intercalate and form lamella, which effectively 'glue' the NPs together in various packed arrangements. We believe that a similar process is occurring with our ZnO NPs, leading to self-assembly of the observed nanoleaf structures.

Figure 3(e) shows the UV–visible optical absorption spectra of the suspensions following different ablation times in 0.05 M SDS. The peak around 350 nm is attributed to the exciton absorption of ZnO [10]. The peak intensity increased with the increase of *t*; however, the peak for 2 h has a broad shoulder and is poorly defined. Using the value for onset of absorption (where the extrapolation of the steeply rising part of the absorption spectrum crosses the wavelength axis), the optical (or Tauc) bandgap [24] for samples produced after 2 and 5 h ablation are calculated to be 3.20 and 3.10 eV, respectively. These two values are lower than the value for bulk ZnO (3.37 eV) [19] probably due to quantum confinement effects.

Figure 3(f) summarizes a suggested mechanism that is consistent with our observations, by which the ZnO particles might self-organize (0D → 1D → 2D) into the observed complex structures. The high power laser beam causes material to be ejected from the zinc plate predominantly as atomic or ionic species, resulting in the formation of a high temperature, high pressure, and high density (HTHPHD) plasma of evaporated materials. The highly energetic Zn species created within the ablation plume are easily oxidized in such extreme conditions, and then initially condense into small monodispersed spherical ZnO NPs. Due to the very short laser pulse length (15 ns) and the fact that the plume is rapidly quenched by the surrounding liquid, the growth times of these nuclei are very short, and so they remain in the nanometre size range. At a short ablation time, the rate of mesoscale restructuring is relatively low because of insufficient energy input to overcome the restructuring barrier. Thus, the initial products are mainly spherical NPs. However, more complex assembled structures are formed in a longer ablation time (5 h), which has continual energy input to the reaction system and sufficient time for NPs recrystallization. Furthermore, the presence of SDS molecules can form a thin coating around each NP, stabilizing them, but also preventing further growth since all the crystal faces will be capped by the surfactant groups. At higher SDS concentrations the tail groups protruding from neighbouring NPs begin to intercalate, thereby minimizing the tail–water interactions, and gluing the NPs together. The NPs lying parallel to the *c* axis are stabilized by SDS to give preferential growth along the [0001] direction. Upon drying of the samples, the strings of NPs coalesce to form the nanoleaf structures. The binding of SDS on the NP surfaces directs their subsequent oriented assembly and growth. This surfactant-mediated restructuring process is consistent with the mechanism proposed by several groups for

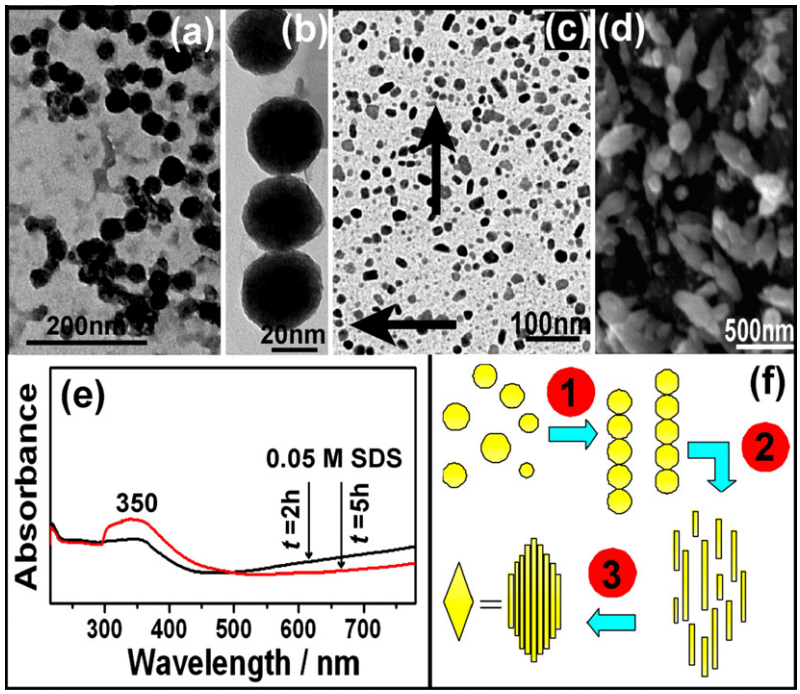

Figure 3. (a) and (b) the aligned packing of the NPs (0.001 M SDS, $t = 2$ h), (c) the particles lining up, serving as the starting point for subsequent coalescence into a NR (0.05 M SDS, $t = 2$ h), (d) leaf-like structures (0.05 M SDS, $t = 5$ h), (e) plot of UV–visible absorbance from the ablation product (0.05 M SDS) for different ablation times, showing a prominent feature at ∼350 nm. (f) Proposed model for sequential growth pathway.

other materials [25, 26]. In general, many surfactants influence crystal morphology by selective interaction or adsorption on certain faces of the growing crystals, which results in preferential growth along other crystallographic directions. It is still unclear why the NPs form 1D lines rather than random 3D clumps. Further investigations (such as varying the laser fluence, the effect of pH and the conditions for the drying process) are required to elucidate the more detailed aspects of ZnO growth in LP-PLA.

Figure 4 compares room temperature PL spectra from four ZnO samples ablated under different SDS concentrations. All the spectra show conventional Raman modes similar to those of bulk ZnO and common nanostructured ZnO [27, 28]. The UV emission is well understood as near-band-edge emission, while the visible emission originates from a variety of deep level defects, e.g. vacancies from oxygen and zinc interstitials. The PL spectrum (figure 4(a)) from the 0.001 M SDS sample shows a small UV emission peak at ∼377 nm and a dominant, broad green/yellow visible emission. The intensity of emission peaks in the blue region increased with increasing SDS concentration together with a slight redshift. Conversely, the reduced green emission with the increase of SDS concentration can be attributable to a decrease of oxygen vacancies within the ZnO. That is because SDS molecules can significantly suppress the oxidation rate by forming extremely thin organic layers on the particle surface. The present PL studies indicate that an evolution in ZnO structure (i.e. 0D → 1D → 2D) changed the distribution of UV emission and visible emission intensities. An identical sample (a), after annealing at 200 °C for 2 h, showed a large (∼6×) increase in the UV emission intensity and a concomitant quenching of the visible

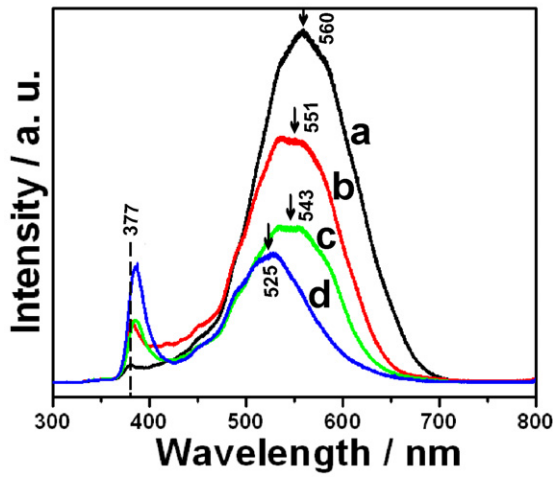

Figure 4. PL spectra obtained from 325 nm excitation of the sample following 2 h laser ablation with SDS concentrations of: (a) 0.001 M, (b) 0.01 M and (c) 0.05 M. (d) Sample identical to (a), but after annealing for 2 h at 200 °C in an oven in air.

emission. The evident reduction in long wavelength emission intensity from the annealed sample serves to reinforce previous suggestions [29] that oxygen-related defects, such as oxygen interstitials, are responsible for the yellow and red emission.

4. Conclusions

In summary, ZnO nanoleaf structures can be self-assembled using simple, room-temperature, solution–solid phase reactions. This work has shown that LP-PLA is an effective method to

synthesize a series of nanomaterials with controlled size and morphology. PL from different samples confirmed annealing as a good route to improving the intensity of UV emission from the sample. Factors such as surfactant concentration near the cmc and longer reaction times are favourable in defining the structures observed here.

Acknowledgments

This work was supported by Universities UK via the Overseas Research Scholarship (ORS) scheme and the University of Bristol. The authors thank J Jones, Dr J A Smith, K N Rosser, Dr Z S Song and Y Sun for their many and varied contributions to the work described herein.

References

[1] Yang G W and Wang J B 2000 *Appl. Phys.* A **71** 343
[2] Liang C H, Shimizu Y, Masuda M, Sasaki T and Koshizaki N 2004 *Chem. Mater.* **16** 963
[3] Yang L, May P W, Yin L, Smith J A and Rosser K N 2007 *Diamond Relat. Mater.* **16** 725
[4] Wang J B, Yang G W, Zhang C Y, Zhong X L and Ren ZH A 2003 *Chem. Phys. Lett.* **367** 10
[5] Simakin A V, Voronov V V, Kirichenko N A and Shafeev G A 2004 *Appl. Phys.* A **79** 1127
[6] Shafeev G A, Freysz E and Bozon-Verduraz F 2004 *Appl. Phys.* A **78** 307
[7] Sylvestre J P, Poulin S, Kabashin A V, Sacher E, Meunier M and Luong J H T 2004 *J. Phys. Chem.* B **108** 16864
[8] Dolgaev S I, Simakin A V, Voronov V V, Shafeev G A and Bozon-Verduraz F 2002 *Appl. Surf. Sci.* **186** 546
[9] Usui H, Shimizu Y, Sasaki T and Koshizaki N 2005 *J. Phys. Chem.* B **109** 120
[10] Zeng H B, Cai W P, Cao B Q, Hu J L, Li Y and Liu P S 2006 *Appl. Phys. Lett.* **88** 181905
[11] Liu J P, Huang X T, Li Y Y, Sulieman K M, Sun F L and He X 2006 *Scr. Mater.* **55** 795
[12] Liu B and Zeng H C 2004 *J. Am. Chem. Soc.* **126** 16744
[13] Yang L, May P W, Yin L, Brown R and Scott T B 2006 *Chem. Mater.* **18** 5058
[14] Yang L, May P W, Yin L, Scott T B, Smith J A and Rosser K N 2006 *Nanotechnology* **17** 5798
[15] Yang L, May P W, Yin L, Smith J A and Rosser K N 2007 *J. Nanopart. Res.* doi:10.1007/s11051-006-9192-4
[16] Yang L, May P W, Huang Y Z and Yin L 2007 *J. Mater. Chem.* **17** 1255
[17] Burke S E and Eisenberg A 2001 *Langmuir* **17** 8341
[18] Liu B and Zeng H C 2003 *J. Am. Chem. Soc.* **125** 4430
[19] Zeng H B, Cai W P, Li Y, Hu J L and Liu P S 2005 *J. Phys. Chem.* B **109** 18260
[20] Mo M, Yu J C, Zhang L and Li S-K A 2005 *Adv. Mater.* **17** 756
[21] Wang X F, Xu J B, Ke N, Yu J G, Wang J, Li Q, Ong H C and Zhang R 2006 *Appl. Phys. Lett.* **88** 223108
[22] Penn R L and Banfield J F 1998 *Science* **281** 969
[23] Sasaki T, Shimizu Y and Koshizaki N 2006 *J. Photochem. Photobiol.* A **182** 335
[24] Tauc J 1974 *Amorphous and Liquid Semiconductors* (London and New York: Plenum) p 171
[25] Yu J G, Zhao X F, Liu S W, Li M, Mann S and Ng D H L 2007 *Appl. Phys.* A **87** 113
[26] Chen D, Shen G Z, Tang K B, Liang Z H and Zheng H G 2004 *J. Phys. Chem.* B **108** 11280
[27] Sun Y, Fuge G M, Fox N A, Riley D J and Ashfold M N R 2005 *Adv. Mater.* **17** 2477
[28] Zhang Y, Jia H B, Wang R M, Chen C P, Luo X H, Yu D P and Lee C J 2003 *Appl. Phys. Lett.* **83** 4631
[29] Cross R B M, De Souza M M and Narayanan E M S 2005 *Nanotechnology* **16** 2188